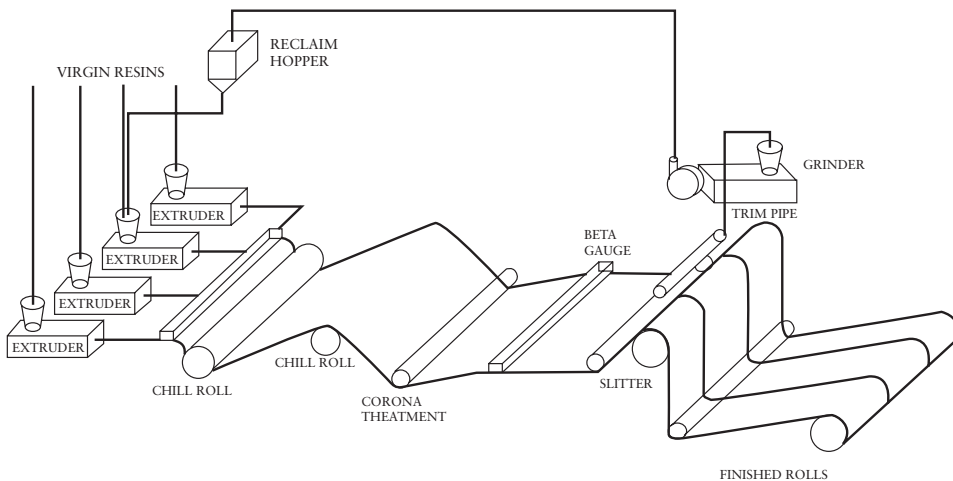


# 4 Flat Film and Sheet Dies

J. Vlachopoulos, N. Polychronopoulos, S. Tanifuji, J. Peter Müller

## 4.1 Film Casting and Sheet Extrusion

In flat film or sheet production the first objective is to spread a continuous polymer melt stream coming from an extruder into a die, which terminates in a rectangular and wide cross-section, having a small gap. After the die the molten extrudate is cooled on chilled rollers and solidifies, as shown in **Figure 4.1**. The figure also shows corona treatment to render the surface more receptive to inks, adhesives or other coatings, beta gauge for measuring the thickness and trim reclaim. Products of less than 0.25 mm in thickness are referred to as films and those over 0.25 mm are referred to as sheets [1].



**Figure 4.1** A four-layer cast film line. Adapted from J. Ivey in *The SPE Guide on Extrusion Technology and Troubleshooting*, Eds. J. Vlachopoulos and J. Wagner, Society of Plastics Engineers, Brookfield, CT, USA, 2001, 12.1 [1]

The rate at which the extrudate is cooled determines several important properties of the finished product. Longer cooling means there is more time available for crystal growth and thus the crystallites will be larger [2]. Crystallinity affects the density, optical properties, coefficient of friction, impact, barrier and other properties. Compared to blown film, the cast film process shows better optical properties, higher output rate per hour, lower gauge variation and lower converting cost. Most cast film lines manufactured today are coextrusion lines and in fact **Figure 4.1** shows a four-layer line. Coextrusion is defined as the process of simultaneous extrusion of two or more materials through a common die. It is used for the purpose of combining material properties and reducing the cost at the same time. Thickness uniformity in monolayer extrusion and layer uniformity in coextrusion are the key measures for quality.

Sheet lines, as noted earlier, are lines that produce film with a thickness exceeding 0.25 mm. Typically a sheet line will have a three-roll coating stack after the die, as shown in **Figure 4.2**, and again the cooling rate plays a very important role in determining the properties of the finished product. A detailed troubleshooting guide of monolayer and coextruded sheet is available in the open literature [3]. Several issues relating to film processing, materials and properties are discussed in a handbook [4].

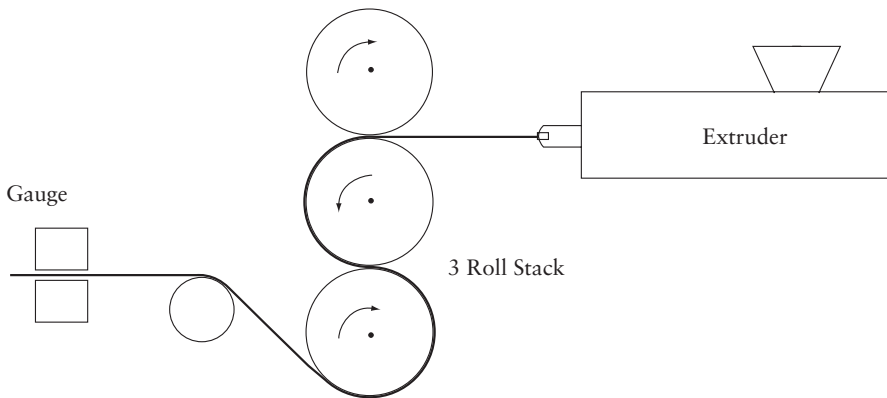


**Figure 4.2** Sheet extrusion line

## **4.2 Flow Distribution and Channel Design**

The molten polymer stream coming from an extruder must be distributed as uniformly as possible into a rectangular shaping area so that a thin wide sheet or film of uniform thickness is produced continuously. Between the melt pipe, coming from the extruder, and the rectangular die lips a distribution channel (usually called

a manifold) is needed. The most common dies [5-8] utilise either the simple ‘T-slot’ or the ‘coathanger’ geometry. T-slot dies are the simplest to manufacture. They have a large manifold of usually circular cross-section, which is constant across the entire width of the die, as shown in **Figure 4.3**. There is very little resistance to flow from the centre (feed) to the side ends of the die and even flow distribution is accomplished by the flow controlling action of the die lips. Such dies are used for low viscosity polymers (high melt flow index resins) mainly for extrusion coating applications. A less common type of die is the ‘fishtail’ design, shown schematically in **Figure 4.4**. Coathanger dies usually involve [5] a manifold, a preland, possibly a flow restrictor (also called a ‘choker bar’), a secondary manifold and finally the primary land (die lips) as shown schematically in **Figure 4.5**. A picture of the lower half of a modern flat die is shown in **Figure 4.6**.

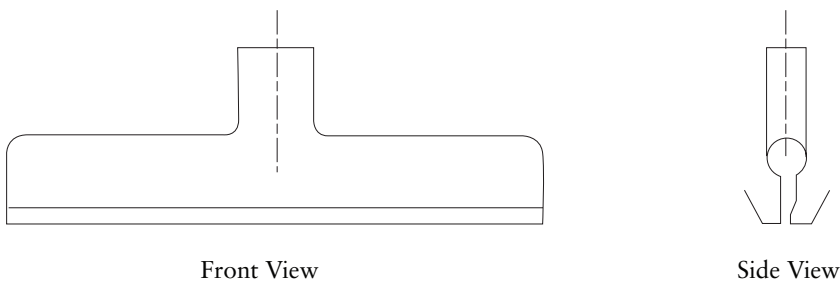


**Figure 4.3** T-slot die with a constant cross-section circular manifold. Adapted from D.R. Garton in *Film Extrusion Manual*, Eds., T.I. Butler and E.W.Veazey, TAPPI, Atlanta, GA, 1992, p.231 [5]

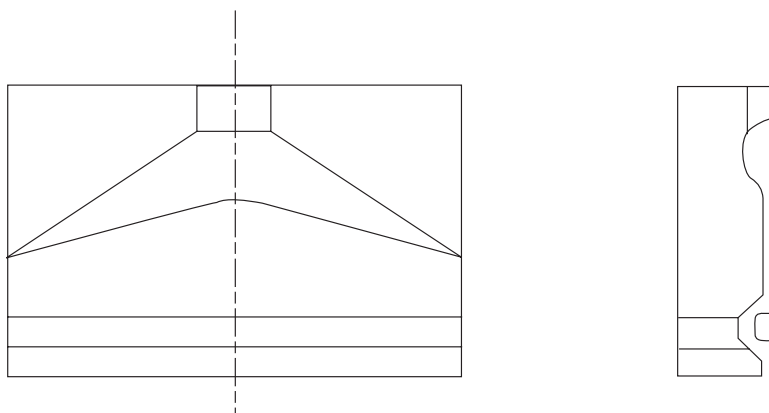


**Figure 4.4** Fishtail die. Adapted from W. Michaeli, *Extrusion Dies for Plastics and Rubber*, 2<sup>nd</sup> Edition, Hanser Publishers, Munich, 1992 [6]

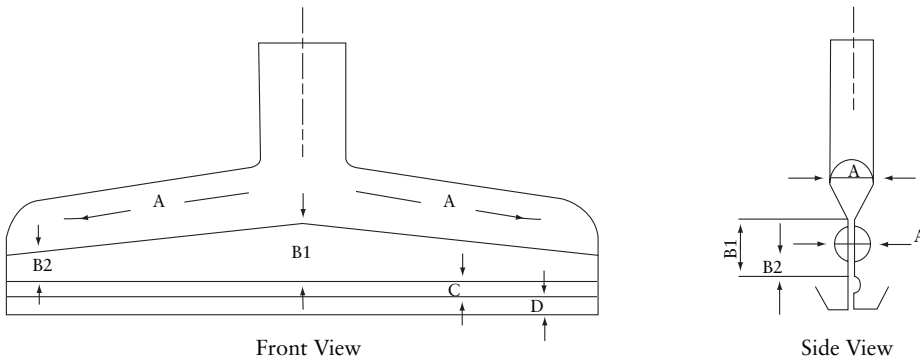


**Figure 4.5** Coat hanger die having a teardrop shaped manifold with a diminishing cross-sectional area from the centre to the sides. A region is the manifold, B1 and B2 are lengths of the preland, C is a secondary manifold and D the land (die lips). Adapted from D.R. Garton in *Film Extrusion Manual*, Eds., T.I. Butler and E.W.Veazey, TAPPI, Atlanta, GA, 1992, p.231 [5]

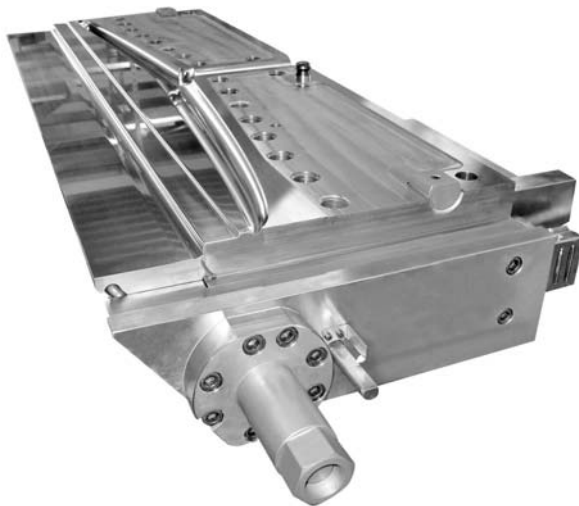


**Figure 4.6** Picture of the lower half of a modern flat die having a lower sliding lip, which can be adjusted during production. Reproduced with permission from EDS GmbH, Kirchdorf, Austria

The manifold cross-sectional area is frequently teardrop shaped (see **Figure 4.7**) and is gradually reduced from the centre (feed) to the side ends. Rectangular manifolds (see **Figure 4.7**) are used in coextrusion and again the cross-sectional area is reduced from the centre to the sides. The function of the manifold is to force the polymer to the sides and downstream at the same time for the generation of a nearly uniform flow distribution by the end of the preland, so that the necessity for subsequent corrections is minimised. The shape and the dimensions of the manifold are crucial in designing a die capable of producing a film or sheet of uniform cross-section from the die lips. Teardrop shaped manifolds have evolved over the years from flat back to curved back, as shown in **Figure 4.8**. The most common manifold design by far, in the current market, is the straight backline. More sophisticated designs involve a parabolic backline in combination with a parabolic shaped preland, as shown in **Figure 4.9**. This design is known to reduce what is usually referred to as the ‘M’ or ‘W’ flow output problem of the film or sheet produced, being heavy on each end then having a thin area followed by a thick area in the centre (which can be perceived as having the shape of the letter W or an inverted one).



**Figure 4.7** Common types of manifold cross-sections

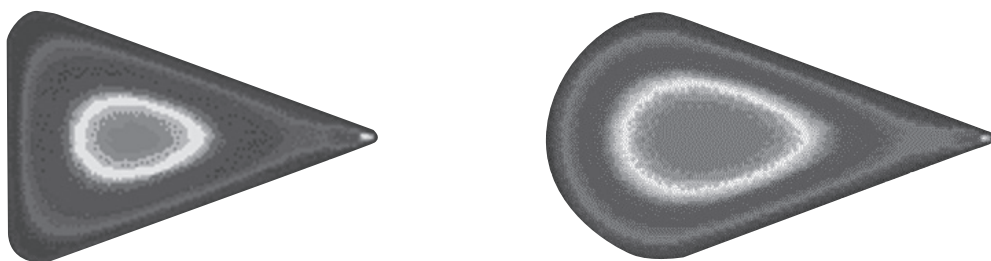


**Figure 4.8** Evolution of the teardrop manifold shape from the older flat back (left) to the modern curved back (right). The highest velocity is in the centre and the lowest on the walls

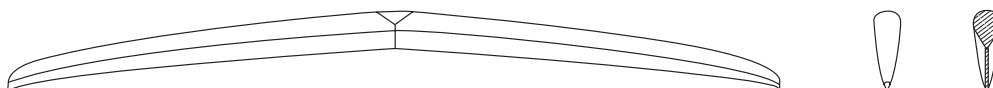


**Figure 4.9** Parabolic backline manifold and preland

Most flat dies include some kind of lip-adjusting systems for fine-tuning of the uniformity. These might be simple adjusting screws or very sophisticated arrangements involving thickness measurement and feedback control. However, these adjusting systems are not capable of correcting large flow nonuniformities which result from poor manifold and preland design. All channel sections must be streamlined, as much as possible, and capable of providing smooth melt flow without any stagnating or recirculating flow regions. A mechanical drawing of a cross-section of a die having a restrictor bar and lip adjustment is given in **Figure 4.10**.

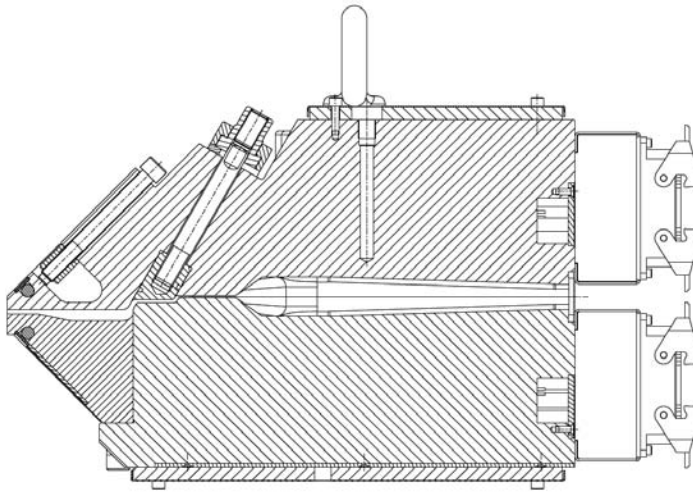


**Figure 4.10** Cross-sectional area of a die having a restrictor bar and a lip adjustment system. Reproduced with permission from EDS GmbH, Kirchdorf, Austria

Flat die design practitioners also recommend that for film production (especially if transparent) the minimum wall shear rate must not be less than  $8 \text{ s}^{-1}$ . Low wall shear rates are likely to result in visual defects on the film due to polymer degradation, which may look like brown or black spots, haze bands or even a generalised deterioration of the appearance of the sheet or film. Occasionally, such defects might be confused with sharkskin. The origin, however, is totally different. Sharkskin occurs at the die lip exit as discussed in [9, 10] and **Chapter 1** of this book. The low wall shear rate effect originates upstream where the flow channels are deep and consequently the corresponding shear rates may be very low. The previously mentioned minimum wall shear rate value of  $8 \text{ s}^{-1}$  has been known and quoted by die designers for several years, even before the extensive use of computer simulation tools, which make possible the accurate determination of the shear rate for a given geometry and given flow rate. Due to long residence times and some sort of sticking of the polymer melt at the die surface, chain scission, cross-linking or other thermal degradations may occur. Some temperature sensitive polymers, notably ethylene-vinyl alcohol (EVOH), polyvinyl chloride (PVC), polyvinylidene chloride and ethylene-vinyl acetate (EVA), are particularly susceptible to this defect. For such materials, the minimum required wall shear rate value to avoid degradation is probably higher, but there have not been any published studies about this available in the open literature. In coextrusion, the EVOH or the EVA layer may contain defects as a result of this sort of degradation,

but the other layers could be defect-free, even though low wall shear rates might be encountered in all layers. In such a case, the degradation of the temperature sensitive layer might be confused with interfacial stability [10, 11], which is discussed later in this chapter.

In addition to good flow channel design, it is important that the die body be free from temperature variations during production. Locally higher temperature is likely to produce a heavy-gauge band, due to higher flow rate, while a locally lower temperature is likely to produce a thin-gauge band. Insulation and temperature control of the die body are essential for achieving film or sheet with low thickness tolerances. Flat dies are usually manufactured in widths ranging from 700 mm to 3,500 mm but may occasionally exceed 5000 mm. Film or sheet thicknesses usually range from 10  $\mu\text{m}$  to 30 mm. Deckling systems are used to reduce the width of film or sheet produced. As Garton [5] put it, they are considered a necessary evil in the industry. They compromise the flow distribution because of the restrictions on the two sides of the die. They should definitely be avoided when extruding thermally degradable polymers. Garton [5] recommends that no more than 25% of the total die width should be deckled. Despite the fact that deckling systems do not produce anything resembling a streamlined flow (which is dictated by rheology), many dies are deckled down to almost 50% of the original slot width.

Due to the large forces that may develop during extrusion and because a flat die is clamped together at the edges, deflection of the die may occur with the largest magnitude at the centre. This is usually referred to as clamshelling. It results in increased flow in the central region, which must be compensated for through lip adjustments.

### **4.3 Mathematical Modelling**

Carley [12] was the first to develop design equations for T-shaped dies assuming Newtonian flow behavior. Pearson [13] extended the design equations to power law fluids. McKelvey and Ito [14] proposed as the design objective the uniformity of flow rate across the die width. These early approaches are elucidated and explained by Tadmor and Gogos [15]. A design method focusing on the distribution problem was proposed by Winter and Fritz [16].

Vlcek and co-workers [17] developed a control volume approach and a software package for flow simulation as the polymer melt spreads laterally and flows downstream. This approach enabled the examination of alternatives, such as the shape of the manifold, flow restrictions and temperature effects. These authors also presented comparisons to experimental data for a small laboratory, die.

For simulation of polymer melt flow through the channels of a flat die, the equations of conservation of mass, momentum and energy under creeping flow conditions (Reynolds number  $\ll 1$ ) must be solved simultaneously. Pressures can reach perhaps 40 MPa in flat die extrusion and this suggests density and viscosity increases. While the effect of pressure on melt density is small (perhaps 5% under the most severe extrusion conditions) the effect on viscosity is larger. Cogswell [18] suggests as a very rough estimate that a pressure of 10 MPa has as much effect as a reduction of 5°C in temperature. Recent measurements by Halasz and Huszar [19] also show that viscosity increases significantly in the usual pressure range of die extrusion. While the viscosity dependence on temperature is nearly always taken into consideration, the authors are not aware of any serious attempts to consider pressure dependence of viscosity in extrusion die design. Thus, in the presentation below, the incompressibility assumption will be used and the viscosity will be a function of temperature and shear rate, but not of pressure.

Equation of conservation of mass:

$$\nabla \cdot \bar{V} = 0 \quad (4.1)$$

Equation of conservation of momentum:

$$-\nabla P + \nabla \cdot \bar{\tau} = 0 \quad (4.2)$$

Equation of conservation of energy:

$$\rho c_p \bar{V} \cdot \nabla T = k \nabla^2 T + \bar{\tau} : \nabla \bar{V} \quad (4.3)$$

where  $\bar{V}$  is the velocity vector,  $P$  pressure,  $\bar{\tau}$  stress tensor,  $\rho$  density,  $c_p$  specific heat capacity,  $T$  temperature,  $k$  thermal conductivity and the term  $\bar{\tau} : \nabla \bar{V}$  represents the frictional heating (viscous dissipation). The stress tensor is usually expressed in terms of the generalised Newtonian fluid model (GNF) in the form:

$$\bar{\tau} = \eta(\Pi_D) 2\bar{D} \quad (4.4)$$

where  $II_D$  is the second (scalar) invariant of the strain rate tensor  $\overline{\overline{D}}$  (with double bars) (given in **Figure 4.11**).

$$\overline{\overline{D}} = \frac{1}{2}(\nabla\overline{V} + \nabla\overline{V}^T) = \frac{1}{2}\left(\frac{\partial V_i}{\partial x_j} + \frac{\partial V_j}{\partial x_i}\right) \quad (4.5)$$

The above simplify to:

$$2D_{yx} = \frac{dV_x}{dy} = \dot{\gamma} \text{ (shear rate)} \quad (4.6)$$

$$\eta(II_D) = \eta(\dot{\gamma}) \text{ (viscosity, function of shear)} \quad (4.7)$$

for simple shear flow (e.g., flow between two long flat plates with  $x$  the flow direction and  $y$  the perpendicular).

$$\begin{aligned} \text{Rectangular: } II_D &= 2\left[\left(\frac{\partial v_x}{\partial x}\right)^2 + \left(\frac{\partial v_y}{\partial y}\right)^2 + \left(\frac{\partial v_z}{\partial z}\right)^2\right] \\ &\quad + \left[\frac{\partial v_y}{\partial x} + \frac{\partial v_x}{\partial y}\right]^2 + \left[\frac{\partial v_z}{\partial y} + \frac{\partial v_y}{\partial z}\right]^2 + \left[\frac{\partial v_x}{\partial z} + \frac{\partial v_z}{\partial x}\right]^2 \\ \text{Cylindrical: } II_D &= 2\left[\left(\frac{\partial v_r}{\partial r}\right)^2 + \left(\frac{1}{r}\frac{\partial v_\theta}{\partial \theta} + \frac{v_r}{r}\right)^2 + \left(\frac{\partial v_z}{\partial z}\right)^2\right] \\ &\quad + \left[r\frac{\partial}{\partial r}\left(\frac{v_\theta}{r}\right) + \frac{1}{r}\frac{\partial v_r}{\partial \theta}\right]^2 + \left[\frac{1}{r}\frac{\partial v_z}{\partial \theta} + \frac{\partial v_\theta}{\partial z}\right]^2 \\ &\quad + \left[\frac{\partial v_r}{\partial z} + \frac{\partial v_z}{\partial r}\right]^2 \\ \text{Spherical: } II_D &= 2\left[\left(\frac{\partial v_r}{\partial r}\right)^2 + \left(\frac{1}{r}\frac{\partial v_\theta}{\partial \theta} + \frac{v_r}{r}\right)^2 + \left(\frac{1}{r\sin\theta}\frac{\partial v_\phi}{\partial \phi} + \frac{v_r}{r} + \frac{v_\theta \cot\theta}{r}\right)^2\right] \\ &\quad + \left[r\frac{\partial}{\partial r}\left(\frac{v_\theta}{r}\right) + \frac{1}{r}\frac{\partial v_r}{\partial \theta}\right]^2 \\ &\quad + \left[\frac{\sin\theta}{r}\frac{\partial}{\partial \theta}\left(\frac{v_\phi}{\sin\theta}\right) + \frac{1}{r\sin\theta}\frac{\partial v_\theta}{\partial \phi}\right]^2 \\ &\quad + \left[\frac{1}{r\sin\theta}\frac{\partial v_r}{\partial \phi} + r\frac{\partial}{\partial r}\left(\frac{v_\phi}{r}\right)\right]^2 \end{aligned}$$

**Figure 4.11** The second invariant of the strain rate tensor in rectangular, cylindrical and spherical coordinates;  $v_x$ ,  $v_y$  and  $v_z$  represent the velocity components in the  $x$ ,  $y$  and  $z$  directions

The viscosity is usually expressed in terms of the power law, Carreau-Yasuda and Cross models.

Power law:

$$\eta = K \dot{\gamma}^{n-1} \quad (4.8)$$

where  $K$  is the consistency index (i.e. the value of the viscosity at shear rate  $\dot{\gamma}=1/\text{s}$ ) which is temperature dependent in the same way as zero shear viscosity. The power law exponent is usually not a function of temperature.

Carreau-Yasuda:

$$\eta = \eta_o \left[ 1 + (\lambda \dot{\gamma})^a \right]^{\frac{n-1}{a}} \quad (4.9)$$

Cross:

$$\eta = \frac{\eta_o}{1 + (\lambda \dot{\gamma})^{1-n}} \quad (4.10)$$

where  $\eta_o$  is the zero shear viscosity which is a function of temperature, usually expressed either by an Arrhenius expression, mostly used in polymer physics and rheology.

$$\eta = \eta_{ref} \left[ \frac{E}{R} \left( \frac{1}{T} - \frac{1}{T_{ref.}} \right) \right] \quad (4.11)$$

or simple exponential, mostly used in equipment design

$$\eta = \eta_{ref} \exp[-b(T - T_{ref.})] \quad (4.12)$$

where  $\eta_{ref.}$  is a viscosity measured at a reference temperature ( $T_{ref.}$ ),  $E$  is the activation energy and  $R$  is the gas constant. The temperature sensitivity coefficient  $b$  is usually between 0.01 and 0.1/ $^{\circ}\text{C}$  for most commercial polymers. For high density polyethylene (linear polymer) the value of  $b$  is roughly 0.01, while for low density polyethylene (branched) it may reach 0.03. The parameter  $\lambda$  is a time constant and represents some sort of material relaxation. In the Carreau-Yasuda model,  $\lambda$  determines the shear rate at which a transition occurs from the zero-shear rate plateau to the shear thinning portion of the viscosity curve. In the Cross model, when  $\lambda = 1/\dot{\gamma}$  then  $\eta = \eta_o/2$ . In some simulations  $\lambda$  is considered to obey the same temperature dependence as the zero-shear viscosity and with the same parameters:

$$\lambda = \lambda_{ref.} \exp[-b(T - T_{ref.})] \quad (4.13)$$

Viscoelastic constitutive equations [20] are not used for routine flat die design. Some questions relating to viscoelasticity are discussed in **Section 4.6** below.

The momentum and continuity equations shown above can be easily simplified to the generalised Hele-Shaw approximation with the assumption of narrow gap geometry [21]. It applies to geometries in which the gap varies with position (provided there are not abrupt changes). Newtonian and the GNF models of power law, Carreau-Yasuda and Cross models can easily be incorporated. For die design, if we assume that  $x$  is the direction of flow from the extruder end to the die lips,  $y$  is the lateral direction towards the side ends and  $z$  the perpendicular, we can write the Hele-Shaw approximation as:

$$\frac{\partial}{\partial x} \left( S \frac{\partial P}{\partial x} \right) + \frac{\partial}{\partial y} \left( S \frac{\partial P}{\partial y} \right) = 0 \quad (4.14)$$

The quantity  $S(x,y)$ , called the flow conductance, is defined as:

$$S(x, y) = \int_0^h \frac{z^2 dz}{\eta(x, y, z)} \quad (4.15)$$

where  $h$  is the  $z$ -direction gap.

The primary variable is the pressure and, after finding it, the gapwise average velocity components are given by:

$$\overline{V}_x = -\frac{S}{h} \frac{\partial P}{\partial x} \quad \overline{V}_y = -\frac{S}{h} \frac{\partial P}{\partial y} \quad (4.16)$$

and the full velocity distributions can also be calculated, using:

$$V_x(z) = -\frac{\partial P}{\partial x} \int_0^h \frac{z' dz'}{\eta(z')} \quad V_y(z) = -\frac{\partial P}{\partial y} \int_0^h \frac{z' dz'}{\eta(z')} \quad (4.17)$$

where  $z'$  is a dummy variable of integration. The energy equation can be subsequently used to determine the temperature. This is a very useful approximation because it reduces significantly the complexity required to solve the fully three-dimensional (3D) problem.

#### 4.4 Computer-assisted Flat Die Design

The solution of either the 3D conservation equations or the Hele–Shaw approximation will provide pressure, velocities, temperature and several other quantities, which can be calculated from these. However, this represents only a flow simulation for a chosen geometry of the die (manifold, preland, die lips, etc.). If a suitable equation solver is available, the die designer must first choose the geometry and solve the equations, then update the geometry and continue to carry out simulations iteratively until an updated geometry produces the desired results, within certain pre-imposed constraints. These are usually pressure drop less than a maximum value, flow rate uniformity at the die lip exit with less than 3-4% variation, wall shear rate no less than  $8 \text{ s}^{-1}$  or perhaps higher for some temperature sensitive materials (to prevent degradation of slow moving polymer melt). Of course, other requirements may be imposed and, from the computational predictions, the die designer must decide whether a satisfactory design has been obtained or whether the iterative simulations must be continued.

In a departure from this approach Smith and co-workers [22-24] used the Hele–Shaw approximation and a numerical optimisation procedure to design flat dies with minimum pressure drop and reduced velocity variation across the die exit. Lebaal and co-workers [25], developed a design method involving 3D finite element simulation

and a numerical optimisation strategy to minimise the velocity variation across the die exit and optimise the body temperature distribution.

The use of 3D and nonisothermal simulations in optimisation techniques may lead to prohibitive design cost, due to excessive computer time requirements. Even an experienced die designer may have to update the geometry some 30 to 50 times until all the design requirements are met. Especially, if viscoelastic models were to be introduced, iterations would be needed to solve the viscoelastic problem for each updated flow geometry and other iterations arising from the various nonlinearities, and the simulations repeated again and again until the design specifications were satisfied. Space mapping techniques used in other areas of engineering [26] can be useful. Space mapping can minimise the number of iterations needed for evaluation with a fine model (e.g., fully 3D nonisothermal and perhaps viscoelastic) by optimising surrogates based on a ‘coarse’ model (e.g., the Hele-Shaw isothermal approximation).

Although, the mathematical optimisation approaches appear rational, efficient and intellectually appealing, they have not yet been developed sufficiently for flat die design in industrial applications. The iterative simulation procedure with ‘trial-and-error on the computer screen’ using a suitable equation solver is the present day design practice. The designer is likely to start from the desired product dimensions. Its thickness and width will specify the die width and the lip gap. Sheet or film thinning due to stretching from the die lip exit to final product can easily be incorporated into the design calculations. After the die width and lip gap is decided, the designer must choose from experience or somehow determine the lip length. Longer lips improve the output thickness uniformity at the expense of higher pressure drop. Pressure drop calculations for flow between two flat plates might help a designer choose a satisfactory lip length. The next step is to choose the preland dimensions. As a first guess, the preland can have the shape of an isosceles triangle. The next step is the choice of the shape and dimensions of the manifold. A teardrop shape is preferred for a monolayer die, while rectangular shaped manifolds perform better in feedblock coextrusion [27]. Between the preland and the die lips two other sections might be incorporated: a restrictor (choker bar) and perhaps a secondary manifold, if necessary. The choker bar is an adjustable restrictor of the flow across the die width for correcting die design deficiencies originating from the manifold and preland, or for flow imbalance due to changes in polymer shear thinning or temperature nonuniformities. Choker bars have been used for many years, but they can be sources of problems. Mount [27] is in favour of choker bar elimination through better manifold and overall die design.

The above procedure was used for a simple design example shown in **Figures 4.12-4.15**. The aim was to design a die on the computer screen having 800 mm width and 1 mm gap. The viscosity of the material was assumed to be described by the Carreau-Yasuda model (Equation 4.9) having  $\eta_{ref.} = 16968$  Pa.s,  $T_{ref.} = 210$  °C,  $b =$

0.0316/°C,  $\lambda_{ref.} = 1.224$ ,  $n = 0.317$ ,  $a = 1$  and a melt density of 780 kg/m<sup>3</sup>. The melt is assumed to enter the die manifold at 220 °C and the die walls are kept also at 220 °C. The design constraints were the following: the total pressure drop should not exceed 10 MPa, the output thickness variation should not be larger than 3%, the wall shear stress at the die lips should not exceed 0.14 MPa (to avoid potential sharkskin flow instabilities) and the wall shear rate anywhere in the die should not be less than 8 s<sup>-1</sup> or perhaps higher for some temperature sensitive materials (to prevent degradation of slow moving polymer melt). Of course, to design a flat die strictly obeying a set of predetermined constraints would be a challenging and sometimes impossible task. Some of the constraints have conflicting requirements. Lower pressure and lower shear stress at lip walls imply lower flow rate, while the minimum wall shear rate requirement implies higher flow rate. The die designer must decide whether the simulated performance is satisfactory or the iterative design procedure of choosing a geometry, performing a simulation, inspecting the results and subsequently judiciously modifying the geometry has to be continued. Perhaps some design constraints which are difficult or impossible to satisfy may have to be relaxed. It should be noted here that the theoretical knowledge gained during the design stage can be of significant help for optimising the extrusion process after the die is built. The effects of increasing or decreasing the production rate and wall temperature settings will be known *a priori* and can be used for obtaining a higher output of a better quality product.

The present design process started with some simple calculations of flow between flat plates for 800 mm width and 1 mm gap. It was quickly established that at 200 kg/h the shear stress at the lip wall would be below the often quoted critical value of 0.14 MPa for the onset of sharkskin flow instability. Similarly, on the basis of simple flow calculations the diameter of cylindrical manifold was selected and quickly modified to the teardrop shape, which is known to give the best results for monolayer flat film/sheet extrusion. After the first geometry was chosen, a flow simulation was carried out using the FLATCAD ADVANCE software package [28] which permits easy modification of the flat die geometry. This package uses a finite element solution of the Hele-Shaw flow approximation equations discussed earlier, with the difference that Hele-Shaw is applied layer-by-layer, for ten layers across the gap and with a fully 3D energy equation. By inspecting the results and comparing them to the target constraints specified earlier, we were able to determine some trends, which enabled us to speed up the ‘trial-and-error procedure on the computer screen’ and arrive at the geometry shown in **Figure 4.12**, after several iterations on local geometrical details.

*Design of Extrusion Forming Tools*

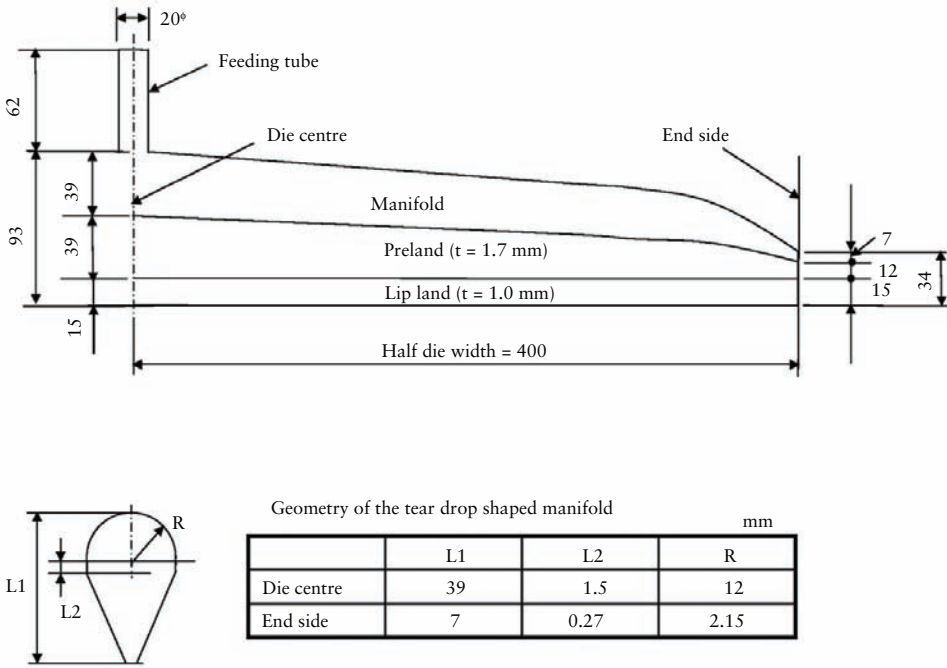


**Figure 4.12** Geometrical specifications of the flat die which was used in the final simulations shown in **Figures 4.13, 4.14** and **4.15**

**Figure 4.13** shows the streamlines of the polymer melt as it spreads to the sides and flows downstream. **Figure 4.14** shows the pressure field and **Figure 4.15** shows the average velocity distribution at the die lip exit.

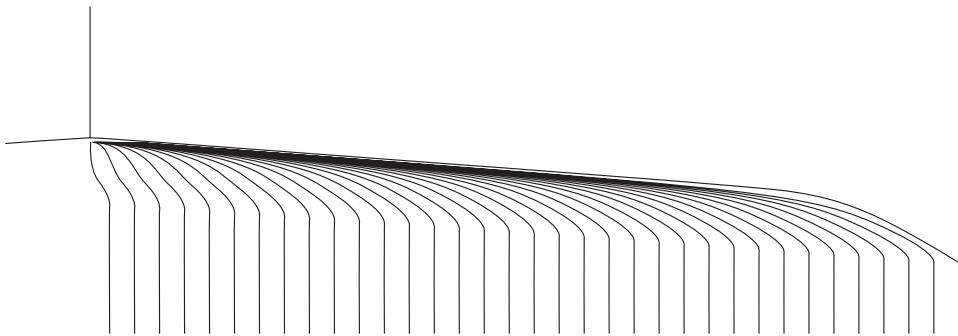


**Figure 4.13** Streamlines predicted by the FLATCAD ADVANCE software package [28], for the die geometry shown in **Figure 4.12**

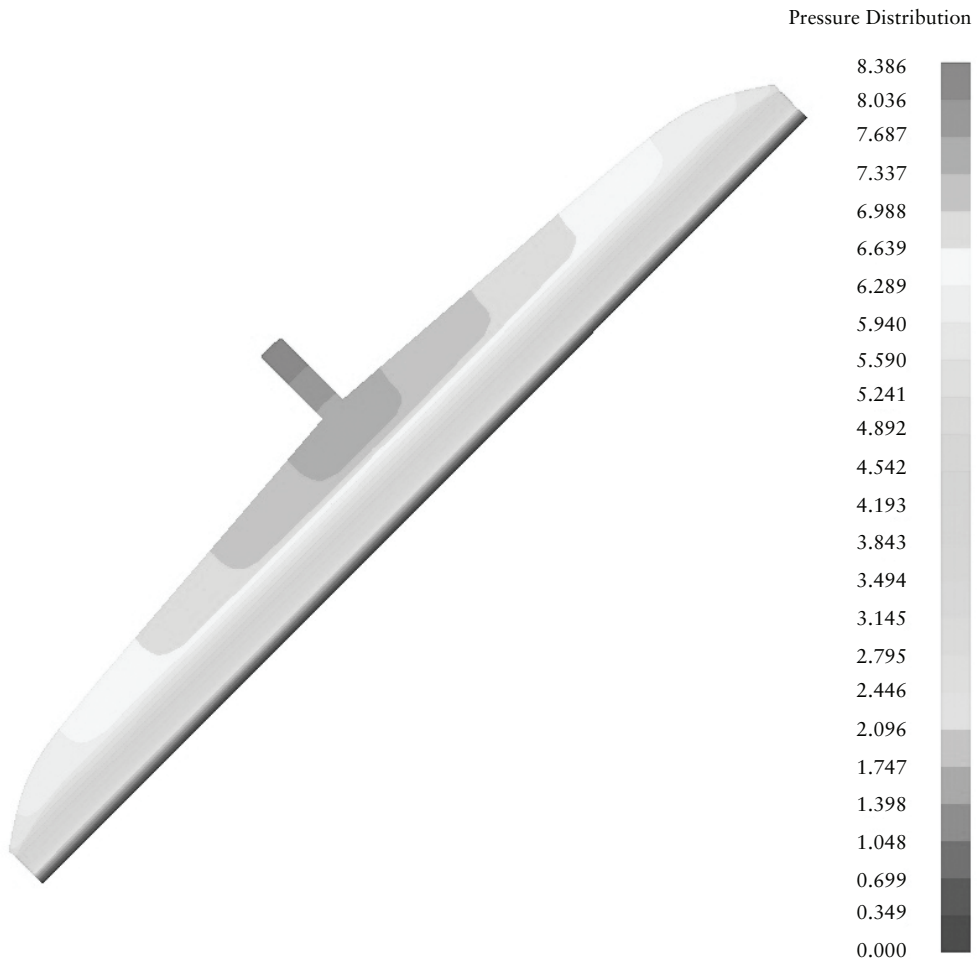


**Figure 4.14** Predicted pressure distribution for the die geometry shown in **Figure 4.12** (200 kg/h)

The maximum pressure drop is 8.4 MPa and die exit average velocity variation is  $\pm 1.35\%$ . Both these quantities are below the preimposed constraints. The maximum shear stress at the exit was 0.116 MPa which is below the critical value of 0.14 MPa for sharkskin. The minimum wall shear rate was located in the manifold near the centre before the preland region, and it was  $7.24 \text{ s}^{-1}$  for a production rate of 200 kg/h, which is slightly below the preset constraint of  $8 \text{ s}^{-1}$ . Taking into consideration the fact that a somewhat larger production rate produces a larger minimum wall shear rate without exceeding the maximum pressure and maximum shear stress requirements,

we decided to stop the iterative design process. The geometry shown in **Figure 4.12** was deemed to be satisfactory.

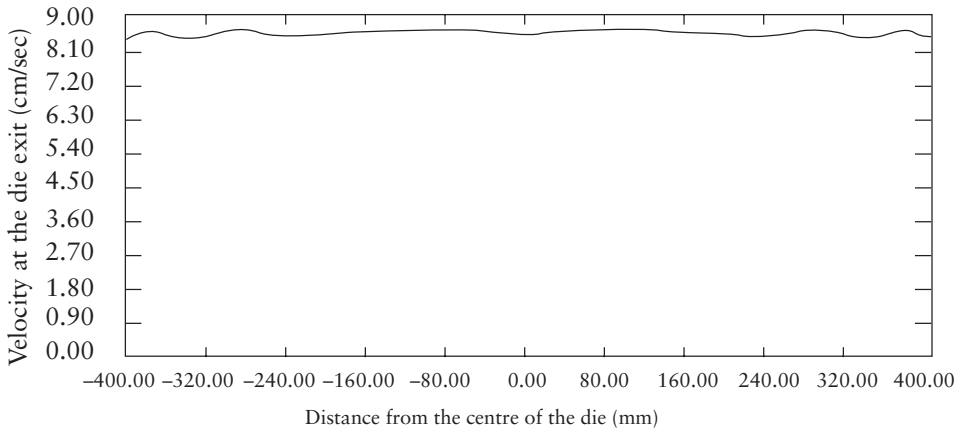


**Figure 4.15** Predicted average velocity distribution at the die exit. Variation  $\pm 1.35\%$

### 4.5 Flat Die Coextrusion

The earliest coextruded sheets and films were produced using multimanifold dies. In this technology the layers are formed individually in separate dies, which have the usual manifold preland and land sections, and then the layers are joined together before the exit (**Figure 4.16a**). There is a limitation with such dies due to geometry and the necessity of having metal walls for each die manifold thick enough for tool integrity and avoidance of nonuniformity arising from clamshelling. While construction is relatively easy for up to three layers, the mechanical complexity and cost increase significantly with each additional layer.

Schrenk and Chisholm [29, 30] developed a new production technology in which, the layers are joined together in a device called a feedblock prior to the die, as shown schematically in **Figure 4.16b**. Then, the layered structure is extruded through a single manifold. Feedblock systems are a lot simpler and easier to manufacture than multimanifold dies. They are also easier to assemble, disassemble, clean, operate

and are more flexible for implementing whatever changes might be necessary. The main challenge in feedblock die coextrusion is the maintenance of layer uniformity, from the feedblock through the spreading in the manifold, flow in the preland and die lips, to the exit. Despite this challenge, feedblock coextrusion is the dominant technology. In fact, by combining multimanifold and feedblock dies (see **Figure 4.16c**) it is possible to produce multilayered films comprising hundreds of layers [31]. This is accomplished in a coextrusion feedblock by first splitting the melt flow, then realigning and subsequently stacking a small number of melt streams.

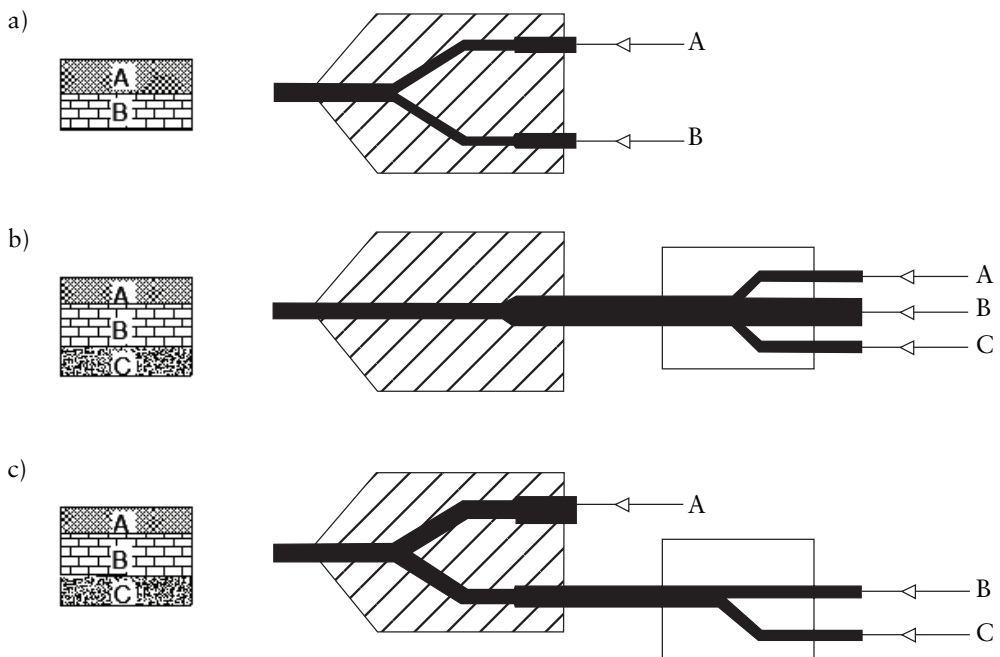


**Figure 4.16** Schematic representation of multilayer extrusion. (a) Multimanifold; (b) feedblock; and (c) combination of feedblock and multimanifold. Adapted from R. Wirtz in *Auslegung von Extrusionwerkzeugen*, VDI Verlag, Düsseldorf, 1996, 72 [7]

Multimanifold dies are used for products which are difficult or impossible to fabricate by means of feedblock coextrusion. These include structures which are required to have very thin skin layers compared to the total thickness and structures with very large viscosity and temperature differences in adjacent layers. The layer nonuniformities

in feedblock coextrusion might be due to encapsulation tendencies of the more viscous polymer by the less viscous one [32]. Feedblock profiling is used for the production of uniform multilayer melt streams by counteracting the encapsulation tendency as shown schematically in **Figure 4.17** adapted from Cloeren [33]. Also, the second normal stress difference, due to polymer viscoelasticity, may give rise to secondary flows [34] and encapsulation phenomena [35]. Mathematical modelling of coextrusion flows is challenging even for inelastic fluids [36, 37] for two layers only. Layer spreading in coextruded structures remains ‘a problem solved more often with art than science’ according to Powers and co-workers [38]. This was true at the time of the cited publication [38] in 2000 and it is true today.

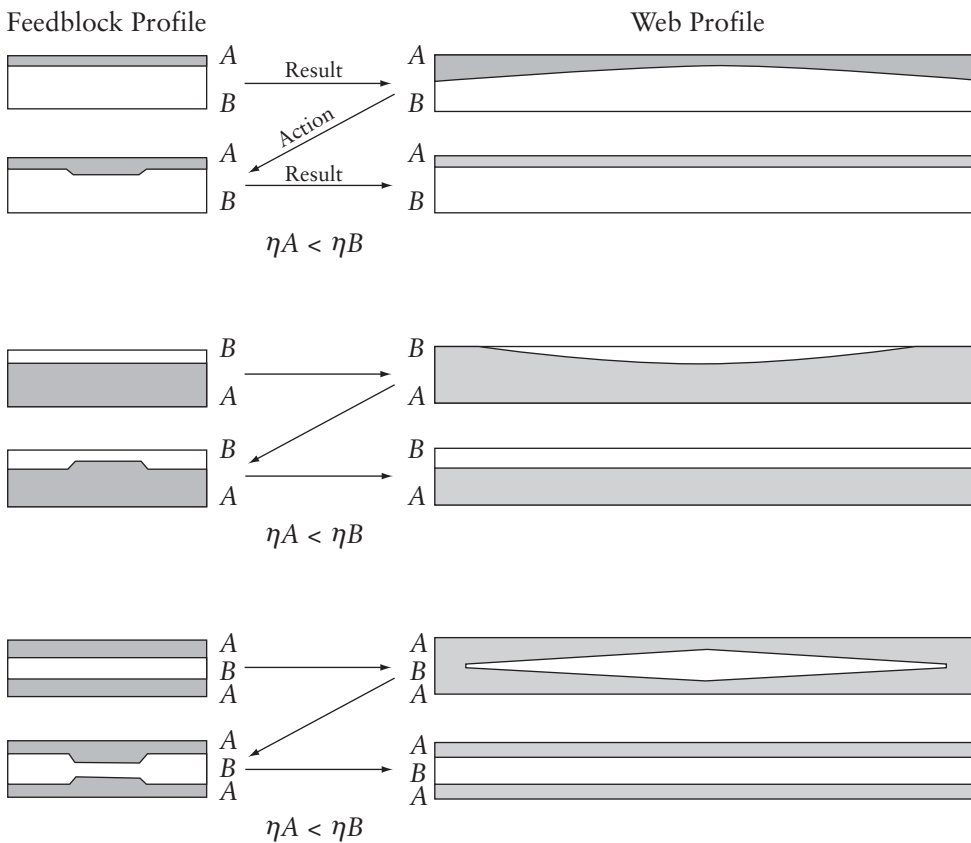


**Figure 4.17** Feedblock profiling and the resultant effects. Adapted from P. Cloeren in *Proceedings of Advances in Extrusion Technology*, RETEC Extrusion Division and the Ontario Section of the Society of Plastics Engineers, Brookfield, NJ, USA, 1993 [33]

In coextrusion, under certain conditions, interfacial instabilities may occur which negatively influence the optical, mechanical and physical properties of the final coextruded products. Some remedies, such as viscosity matching, are not always the solution because even if the same melt is coextruded, instabilities may appear under certain stress and flow conditions. These conditions depend on the rheological properties of the coextruded resins and the flow geometry. There are two types of interfacial instabilities: zig-zag instability and wave pattern instability. Zig-zag instability appears usually as chevrons pointing in the flow direction. It is initiated in the die land and it is characterised by a critical interfacial shear stress, in the range of 40-80 kPa (roughly  $\frac{1}{4}$  to  $\frac{1}{2}$  of the critical wall shear stress for the onset of sharkskin, which is usually quoted as 140 kPa [10]). Optical film clarity is affected significantly by zig-zag instability at the interface. The problems can be remedied by reducing the interfacial shear stress below the critical level. Wave pattern instability appears as a train of parabolas across the width of the sheet and is oriented in the flow direction. It occurs when a fast moving polymer stream merges with a much slower moving stream in a coextrusion feedblock. When the skin layer is thin relative to the second layer, the wave instability can be more pronounced. Large differences in extensional viscosities between adjacent layers can also make the defect more likely. Dies with large lateral expansion ratios (die lip width divided by manifold entry width) seem to be more susceptible [39]. Increased melt elasticity appears to promote these types of instability [40].

## **4.6 Rheological Considerations**

It is easy to show, either with some simple analytical expressions or with a software package, that the outflow rate uniformity (which means the product thickness uniformity) depends on the degree of shear thinning of the polymer melt; the greater the shear thinning the greater the nonuniformity. For the power law model, as the power law exponent becomes smaller the shear thinning and the nonuniformity increase. This means that if a die gives satisfactory nonuniformity (e.g., less than 3-4% in thickness variation) it may not give satisfactory results for a polymer melt having larger shear thinning (i.e., smaller power law exponent). Of course, in industry, the same flat die is likely to be used for extruding different polymers. Thus, during design the above limitation must be taken into consideration and some compromises may have to be made.

The dual nature of polymers, partly viscous and partly elastic, is responsible for several unusual and counterintuitive phenomena [41]. Complex viscoelastic constitutive equations describing the relation between stresses, strains and strain rates must be introduced into the conservation of momentum equation to account for normal stresses, elongational viscosities and stress relaxation effects. Viscoelastic computer

simulations are very challenging even for simple flow geometries, and their predictive power is limited [42]. There have been very limited attempts to simulate flow in flat dies, using viscoelastic constitutive equations. Sun and Gupta [43] took into account elongational viscosity effects in their flat die optimisation. Such effects, however, are believed to be small due to the streamlining that is normally used in flat die channels. Also, normal stress effects may influence the flow pattern in the manifold, or as the melt spreads to the die ends and flows downstream. In addition, the different shear histories experienced by the polymer melt might result in unbalanced frozen-in stresses as the sheet cools at the chill rolls. These in turn may produce warpage in the final product. However, such problems remain academic research objectives and, at present, they are not really taken into consideration using any quantitative methodologies for die design.

Three defects occur after the polymer melt leaves the die lips [44, 45]: draw resonance, neck-in and edge beading. Draw resonance is a periodic fluctuation of film width, thickness and tension. This occurs at a critical draw down ratio (take-up velocity at the chill roll divided by the average velocity at the die exit). Neck-in is the contraction of the lateral width of the extruded web due to the tension imposed by the chill roll. Edge beading (or dog bone effect) is due to the film edges undergoing extension while the neck-in phenomenon is occurring. Edge beads must be trimmed off before film products are collected in rolls. The above defects are responsible for reduction in productivity. Apparently, the melt rheological properties play a significant role in their formation and the die designer must be aware of their potential occurrence.

## **4.7 Mechanical and Other Construction Considerations**

One of the problems of flat dies is their susceptibility to clamshelling, which means deflection of the lips mainly in the centre. This can have a significant influence on the flow distribution and film/sheet thickness nonuniformities. Coathanger designs are particularly susceptible due to large pressures exerted over large surfaces. Michaeli [6] found that reduction in the die land results in significant decrease in deflection. Sander and Pittman [46] developed a coupled approach, using the Hele-Shaw flow approximation to calculate the pressure from the feed to the die lips, and a two-dimensional thick-plate analysis for the deflection. Gifford [47] coupled a 3D flow analysis with a 3D deflection analysis. Wang and Smith [48] combined Hele-Shaw flow approximation with 3D finite element simulation of die deformation and a shape optimisation algorithm.

The adaptor (which is the part that attaches the die to the extruder), all connections, entrances or exits, must have the best possible mechanical fit and match, to provide a smooth flow channel for the polymer melt. Any mismatch will result in material

'hang-ups' and degradation causing random brown or black spots. As mentioned earlier such degradation may also occur in the manifold due to low wall shear rates, when thermally degradable polymers, such as PVC and EVOH, are extruded.

Dies that need to cover a wide range of products and/or process conditions should be equipped with an adjustment device at, or right after, the preland section, which is commonly known as the restrictor bar. Restrictor bars in modern dies are very flexible, allowing for very fine adjustments enabling an even spread of the polymer stream prior to the lip section. The restrictor bar adjustment is done by pushing and pulling. Most systems have push-pull adjusters at each position, and some systems may have one push bolt and one pull bolt at alternating positions. The downside of restrictor bar systems can be material hang-up, degradation and leakage issues. However, this is a proven and commonly used technology, especially in the sheet industry where a large range of materials, with very different viscosities, are processed at varying throughputs and thicknesses.

The final gauge, orientation and surface quality of the film or sheet are provided by the die lips, which usually consist of a back section and a front section, commonly known as the final land. The back section of the lip is usually designed with a larger gap, allowing the material to relax, prior to entering into the final lip land section. Special attention must be paid to the surface of the final lip land, lip face and final lip edge radius. A defined, uniform lip edge radius is needed, especially for high quality optical film and sheet such as polycarbonate or polyethylene terephthalate. High quality surfaces are known to minimise die lip build-up [49] (also known as die drool). For best possible results this final land section should be kept as parallel as possible during the process. Modern die designs include a sliding lower lip which can be adjusted during production by a single point adjustment up to a range of as much as 10 mm keeping the lip absolutely parallel. This can be used to control the die lip build-up and extrudate swell phenomena [49, 50] and leads to a less frequent need to clean the die.

A flex-lip, if present, should be used for fine gauge adjustments, and not for correcting basic uneven flow distribution, or for large changes in lip opening. The standard flex-lip has manual push-only adjusters. For film and extrusion coating it is the industry standard to replace the manual lip adjusting system with an automatic one. There are several different systems available. The standard system utilises thermal bolts, incorporating a heater in each one of them. This system works in combination with a thickness gauging system which has feedback control. By heating, the thermal bolts expand and push down on the flex-lip. By cooling, the bolts contract and open the flex-lip. For more information about flexible adjusting systems the reader is referred to **Chapter 7** of this book.

Perhaps 80% of all of flat dies are manufactured from high temperature tool steel such as P20 (USA) and 1.2311 (Europe). For special applications, higher grade steel is required. It is widely believed that most polymers have a higher tendency to stick to the wall of nonplated stainless steel dies and because of this, more and more dies are plated today. The most common plating is chrome and it is frequently applied on to the surface in multilayer fashion to minimise the existence of microcracks and pores. Chromium nitride plating has become more popular in recent years due to its high hardness, resistance to oxidation and corrosion and very good release characteristics. Chemical nickel platings are only used for processes in which high chemical corrosion occurs.

In most modern dies, both die halves are temperature controlled individually using a larger number of temperature control zones than in the past. This has proven to be a big benefit for most process applications. Lip heaters or liquid temperature controlled lips are necessary for some special applications, such as foamed products.

#### **4.8 Concluding Remarks**

The design of flat dies for film or sheet has evolved over the years from trial-and-error techniques on the factory floor into computer assisted methodologies. The equations of conservation of mass, momentum and energy are solved for creeping flow of non-Newtonian (shear thinning) fluids to predict velocities, pressure, temperature, shear rates and shear stresses. Usually the Carreau-Yasuda and the Cross models of viscosity are used for such simulations. Viscoelastic constitutive equations have attracted considerable interest from academic research workers, but they are not used for industrial design purposes. The current practice of flat die design is through iterative simulation procedures. The trial-and-error techniques moved from the factory floor to the computer screen. The designer will stop the iterative procedure when certain constraints are satisfied. These are usually pre-imposed on the basis of previous experience with the material which is to be extruded, and include a maximum allowable output film/sheet thickness variation, a maximum wall shear stress at the die lip walls, a minimum wall shear rate on the die wall and a maximum pressure drop. Some mathematical optimisation procedures have been developed by academic researchers but, thus far, they have had no impact on flat die design technology.

The T-slot geometry is used for low viscosity materials and coating applications and coathanger shaped dies are used for most other situations. By far the most common designs have a straight backline; more sophisticated designs have a parabolic backline. Modern flat dies are designed with teardrop shaped manifolds having a curved back. Rectangular manifolds are preferable in feedblock coextrusion. After the manifold, a preland, a flow restrictor, a secondary manifold, a lip land and lip adjustment

might be present for obtaining a minimum of thickness variation and high quality output. It should be pointed out that the manifold design is absolutely crucial in achieving an even melt flow distribution, which is necessary to provide a final film or sheet of uniform thickness. The downstream corrections, through a restrictor or lip adjusting systems, are for relatively minor improvements in output uniformity. Although deckling systems, which obstruct the outflow from the die sides, are against rheological principles, they are frequently used in industry for obtaining a sheet or film of the desired width.

## **Acknowledgments**

The authors wish to express their gratitude to T. Nakamura of Polydynamics Inc. (Japan) for carrying out the iterative computer simulations necessary for arriving at the final dimensions of the design example discussed in this Chapter.

## **References**

1. J. Ivey in *The SPE Guide on Extrusion Technology and Troubleshooting*, Eds. J. Vlachopoulos and J. Wagner, Society of Plastics Engineers, Brookfield, CT, USA, 2001, p.12.1.
2. K.R. Osborn and W.A. Jenkins, *Plastic Films*, Technomic Publishing, Lancaster, PA, USA, 1992.
3. J. Powers, *Plastics Technology*, 1996, August.
4. T.I. Butler, *Film Extrusion Manual*, 2<sup>nd</sup> Edition, TAPPI, Atlanta, GA, 2005.
5. D.R. Garton in *Film Extrusion Manual*, Eds., T.I. Butler and E.W. Veazey, TAPPI, Atlanta, GA, 1992, p.231.
6. W. Michaeli, *Extrusion Dies for Plastics and Rubber*, 2<sup>nd</sup> Edition, Hanser Publishers, Munich, 1992.
7. R. Wirtz in *Auslegung von Extrusionwerkzeugen*, VDI Verlag, Düsseldorf, 1996, p.72.
8. T. Kanai in *Film Processing*, Eds., T. Kanai and G.A. Campbell, Hanser Publishers, Munich, Germany, 1999, Chapter 14.

9. J.F. Agassant, D.R. Arda, C. Combeaud, A. Merten, H. Muensted, M.R. Mackley, L Robert and B. Vergnes, *International Polymer Processing*, 2006, **21**, 239.
10. J. Vlachopoulos and D. Strutt in *Multilayer Flexible Packaging*, Ed., J.R. Wagner, Elsevier, Amsterdam, The Netherlands, 2010, p.57.
11. H. Mavridis and K.N. Shroff, *Polymer Engineering and Science*, 1994, **34**, 7.
12. J.F. Carley, *Journal of Applied Physics*, 1954, **20**, 118.
13. J.R.A. Pearson, *Transactions and Journal of the Plastics Institute*, 1964, **32**, 239.
14. J.M. McKelvey and K. Ito, *Polymer Engineering Science*, 1971, **11**, 258.
15. Z. Tadmor and C.G. Gogos, *Principles of Polymer Processing*, 2<sup>nd</sup> Edition, Wiley-Interscience, 2006.
16. H.H. Winter and H.G. Fritz, *Polymer Engineering and Science*, 1986, **26**, 543.
17. J. Vlcek, G.N. Mailvaganam, J. Perdikoulis and J. Vlachopoulos, *Advances in Polymer Technology*, 1991, **10**, 309.
18. F.N. Cogswell, *Polymer Melt Rheology*, Woodhead Publishing, Cambridge, UK, 1996.
19. L. Halasz and A. Huszar, *International Polymer Processing*, 2011, **26**, 4403.
20. R.I. Tanner, *Engineering Rheology*, Oxford Engineering Science, Oxford, UK, 2000.
21. J.A. Dantzig and C.L. Tucker III, *Modeling in Materials Processing*, Cambridge University Press, Cambridge, UK, 2001.
22. D.E. Smith, D.A. Tortotelli and C.L. Tucker, *Computer Methods in Applied Mechanics and Engineering*, 1998, **167**, 3-4, 283.
23. D.E. Smith, D.A. Tortotelli and C.L. Tucker, *Computer Methods in Applied Mechanics and Engineering*, 1998, **167**, 3-4, 303.
24. D.E. Smith and Q. Wang, *Journal of Manufacturing Science and Engineering*, Transactions of the ASME, 2006, **128**, 1, 11.

25. N. Lebaal, F. Schmidt, S. Puissant, *International Journal of Materials and Product Technology*, 2010, **38**, 2-3, 307.
26. J.W. Bandler, Q.S. Cheng, S.A. Dakroury, A.S. Mohamed, M.H. Bakr, K. Madsen and J. Søndergaard, *IEEE Transactions on Microwave Theory and Techniques*, 2004, **52**, 1, 337.
27. E.M. Mount III in *Multilayer Flexible Packaging*, Ed., J.R. Wagner, Elsevier, Amsterdam, The Netherlands, 2010, p.57.
28. FLATCAD ADVANCE Software from H.A.S.L., Tokyo, Japan and Polydynamics Inc., Dundas, Ontario, Canada.
29. D. Chisholm and W.J. Schrenk, inventors; Dow Chemical, assignee; US 3,557,265, 1971.
30. W.J. Schrenk, D.S. Chisholm, K.J. Cleereman and T. Alfrey Jr., inventors; Dow Chemical, assignee; US 3,579,647, 1973.
31. J.H. Schut, *Plastics Technology*, 2006, **52**, 3, 54.
32. C.D. Han, *Multiphase Flow in Polymer Processing*, Academic Press, New York, NY, USA, 1981.
33. P. Cloeren in *Proceedings of Advances in Extrusion Technology*, RETEC Extrusion Division and the Ontario Section of the Society of Plastics Engineers, Brookfield, NJ, USA, 1993.
34. J. Dooley, *Viscoelastic Flow Effects in Multilayer Polymer Coextrusion*, University of Eindhoven, The Netherlands, 2002. [Doctoral Thesis].
35. P.T. Yue, C.F. Zhou, J. Dooley and J.J. Feng, *Journal of Rheology*, 2008, **52**, 4, 1027.
36. A. Torres, A.N. Hrymak and J. Vlachopoulos, *Rheologica Acta*, 1993, **32**, 6, 513; correction in *Rheologica Acta*, 1994, **33**, 3, 241.
37. W.A. Gifford, *Polymer Engineering Science*, 2000, **40**, 9, 2095.
38. J. Powers, J. Dooley, C. Reinhardt and G. Oliver in the *Proceedings of ANTEC 2000*, Orlando, FL, USA, 2000, p.51.
39. R. Ramanathan, R. Shanker, T. Rehg, S. Jons, D.L. Headley and W.J. Schrenk in the *Proceedings of ANTEC1996*, Indianapolis, IN, USA, 1996, p.224.

40. M.T. Martyn, R. Spares, P.D. Coates and M. Zatloukal, *Journal of Non-Newtonian Fluid Mechanics*, 2009, **156**, 150.
41. R.B. Bird, R.C. Armstrong and O. Hessager, *Dynamics of Polymeric Liquids*, Volume 1, Wiley, New York, NY, USA, 1987.
42. J. Vlachopoulos and N. Polychronopoulos in *Applied Polymer Rheology: Polymeric Liquids with Industrial Applications*, Ed., M. Kontopoulou, Wiley, New York, NY, USA, 2011, Chapter 1.
43. Y. Sun and M. Gupta, *International Polymer Processing*, 2005, **20**, 4, 380.
44. D. Silagy, Y. Demay and J.F. Agassant, *Journal of Non-Newtonian Fluid Mechanics*, 1998, **79**, 2-3, 563.
45. C. Sollogoub, Y. Demay and J.F. Agassant, *Journal of Non-Newtonian Fluid Mechanics*, 2006, **138**, 76.
46. R. Sander and J.F.T. Pittman, *Polymer Engineering and Science*, 1996, **36**, 15, 1972.
47. W.A. Gifford, *Polymer Engineering and Science*, 1998, **38**, 10, 1720.
48. Q. Wang and D.E. Smith, *Journal of Applied Polymer Science*, 2007, **103**, 6, 3994.
49. J.D. Gander and J. Giacomini, *Polymer Engineering and Science*, 1997, **37**, 1113.
50. J. Vlachopoulos, *Reviews on Deformation Behavior of Materials*, 1981, **3**, 219.